

Neurovascular Coupling and Oximetry During Epileptic Events

***Minah Suh,* Hongtao Ma, Mingrui Zhao, Saadat Sharif,
and Theodore H. Schwartz***

*Department of Neurological Surgery, Weill Cornell Medical College,
New York Presbyterian Hospital, New York, NY*

Abstract

Epilepsy is an abnormal brain state in which a large population of neurons is synchronously active, causing an enormous increase in metabolic demand. Recent investigations using high-resolution imaging techniques, such as optical recording of intrinsic signals and voltage-sensitive dyes, as well as measurements with oxygen-sensitive electrodes have elucidated the spatiotemporal relationship between neuronal activity, cerebral blood volume, and oximetry in vivo. A focal decrease in tissue oxygenation and a focal increase in deoxygenated hemoglobin occurs following both interictal and ictal events. This “epileptic dip” in oxygenation can persist for the duration of an ictal event, suggesting that cerebral blood flow is inadequate to meet metabolic demand. A rapid focal increase in cerebral blood flow and cerebral blood volume also accompanies epileptic events; however, this increase in perfusion soon (>2 s) spreads to a larger area of the cortex than the excitatory change in membrane potential. Investigations in humans during neurosurgical operations have confirmed the laboratory data derived from animal studies. These data not only have clinical implications for the interpretation of noninvasive imaging studies such as positron emission tomography, single-photon emission tomography, and functional magnetic resonance imaging but also provide a mechanism for the cognitive decline in patients with chronic epilepsy.

Index Entries: Epilepsy; ictal; interictal; intrinsic signal; optical imaging; voltage-sensitive dye; oxygen-sensitive electrodes; neurovascular coupling; oximetry; initial dip; BOLD; rat; seizure; human.

* Author to whom all correspondence and reprint requests should be addressed. E-mail: mis2032@med.cornell.edu
Received August 25, 2005; Accepted February 20, 2006.

Introduction

The study of neurovascular coupling examines the relationship between neuronal activity, metabolism, tissue, and blood oxygenation and blood flow. It has been generally accepted that increases in neuronal activity increase the cerebral metabolic rate of oxygen consumption (CMRO₂), leading to an increase in cerebral blood flow (CBF) and cerebral blood volume (CBV) as the brain attempts to perfuse the active neurons with oxygenated hemoglobin (1). It was then shown, using positron emission tomography (PET) of glucose metabolism (a technique with a slow temporal resolution [approximately seconds]; ref. 2) that increases in CBF occurring 1 to 2 s after the onset of neuronal activity provide an oversupply of oxygenated hemoglobin (HbO₂). Therefore, CMRO₂ and CBF are “uncoupled,” causing relative increases in the concentration of HbO₂ compared with deoxygenated hemoglobin (Hbr), which forms the basis of the blood-oxygen-level-dependent (BOLD) signal that can be imaged with functional magnetic resonance imaging (fMRI; ref. 3). More recently, using techniques with higher spatial and temporal resolution, such as optical recording of intrinsic signals (ORIS; refs. 4 and 5), imaging spectroscopy (6,7), oxygen-dependent phosphorescence quenching (8), oxygen-sensitive electrodes (9,10), and fMRI at 1.5- and 4-Tesla (11,12), investigators have examined changes in tissue and blood oxygenation that occur within the first few hundred milliseconds after neurons become active. These studies have demonstrated a rapid decrease in tissue oxygenation, or an increase in Hbr, that precedes the increase in CBF. This “initial dip,” although questioned by some studies (13–15), implies that for a brief period of time after neurons discharge, the brain is mildly ischemic until cerebrovascular autoregulation dilates arterioles to increase CBF.

Epilepsy is an abnormal physiological state that, unlike normal somatosensory processing, places supranormal demands on the brain's autoregulatory mechanisms because of an

enormous increase in CMRO₂ (16). Therefore, the neurovascular coupling mechanisms that apply in the normal situation may not be relevant. Epilepsy is a disease involving recurrent seizures that consist of the paroxysmal, synchronous, rhythmic firing of a population of pathologically interconnected neurons capable of demonstrating high-frequency oscillatory activity (17). Between these “ictal” events, brief paroxysmal short-duration (~100 ms) events occur called “interictal spikes” (18). Prior investigations into neurovascular coupling during epileptic events have demonstrated contradictory results in both animals and humans using autoradiography, PET, and fMRI, all of which are techniques with limited temporal and spatial resolution (19–25). Although an increase in perfusion is universally demonstrated, some studies have shown that perfusion oversupplies metabolism (24–27), whereas others have demonstrated the opposite—namely, inadequate perfusion to meet metabolic demand (19,21–23). Therefore, the relationship between perfusion and oxygenation during the first few seconds after an epileptiform event has remained elusive. This article reviews recent data on neurovascular coupling during epilepsy obtained in vivo using techniques that have high temporal and spatial resolution such as ORIS, oxygen-sensitive electrodes, and voltage-sensitive dyes (VSDs).

Optical Recording of Intrinsic Signals

The intrinsic optical signal (IOS) is a small change in the absorption (or reflection) of light that occurs in neuronal tissue when neurons are activated. These changes can be recorded from various preparations, ranging from a single neuron preserved in vitro (28) to the human brain in the neurosurgical operating room (29). ORIS has been used extensively to map static functional architecture such as orientation and ocular dominance columns in visual cortex, which has led to discoveries such as the pinwheel organization of orientation

columns (30). The origins of the IOS are multiple because neuronal activity induces a cascade of events in the surrounding tissues, each of which can influence the reflection of light. The real power of the IOS arises from the fact that depending on the wavelength of light, the IOS can separately measure changes in CBV, hemoglobin oxygenation, or light scatter (LS) with a temporal resolution of approx 100 ms and spatial resolution of less than 200 μm (31). At isosbestic wavelengths of hemoglobin, where HbO_2 and Hbr reflect light equally (525, 545, 570.5, and 583 nm; corrected for path-length; ref. 5), ORIS measures total hemoglobin (Hbt), which is directly proportional to CBV and CBF, assuming that the concentration of red blood cells remains constant (32,33). At higher wavelengths (600–650 nm), the majority of the signal arises from the oxygenation state of hemoglobin, because Hbr absorbs light with three times the absorption coefficient of HbO_2 (6,34). Therefore, a decrease in light reflection indicates an increase in Hbr. At wavelengths greater than 650 nm, the signal from LS becomes progressively more significant and ultimately dominates the IOS in the near-infrared region ($>800\text{ nm}$), particularly in avascular preparations (6). This component of the signal arises from a combination of movement of sodium and potassium ions in and out of both neurons and glia, associated fluid shifts, and increases and decreases in the volume of the extracellular space as well as the morphology of the vasculature (28,31,34). Conversely to static functional architecture, epilepsy is a dynamic event that changes over time. Events can begin in varying locations and spread horizontally across the cortex via multiple propagation pathways. Whether the IOS is capable of mapping the complex spatiotemporal dynamics of an evolving epileptiform event has been previously investigated in *in vitro* slices of rat cortex (35) and isolated guinea pig whole brain (36) as well as *in vivo* in rat (37), ferret (38–40), and human (41). Although these studies clearly demonstrated that the IOS can identify the site of an interictal spike (IIS) or ictal onset zone, as well as areas of surround-

ing inhibition (38,39), and may even be sensitive to pre-ictal phenomena that can be useful in predicting the onset of seizures (37), the relationship between epileptiform events and CBV or Hbr has only recently been investigated with the temporal and spatial resolution provided by the ORIS (42–44). Additionally, the sensitivity of the IOS to very rapid changes in electrical activity that occur during epileptiform events was not clear.

In a rat model of interictal spikes arising from focal iontophoresis of bicuculline, a γ -aminobutyric acid-A antagonist, Suh et al. (42) demonstrated that each interictal event elicited a rapid focal increase in Hbr (Fig. 1). Unlike the initial dip following normal sensory processing, which lasts only a few hundred milliseconds, this interictal “epileptic dip” lasts as long as 3 to 4 s (Fig. 1). Similarly, the onset latency appears to be quite rapid, often appearing within 100 ms of the event (Fig. 1). Although the existence of this prolonged hemoglobin deoxygenation implies inadequate CBF, the etiology is not from a delay in CBF, because Suh et al. (42) also found an increase in CBV as early as 100 ms after the interictal spike (Fig. 1). However, the slope (dotted line) of the rise in Hbr is steeper than the rise in CBV, indicating that despite the rapid increase in CBF, CMRO_2 was not adequately met (Fig. 2B). Eventually, the maximum increase in CBV becomes greater than Hbr, and at this point, the oxygen signal inverts into a state of hyperoxygenation, equivalent to an increase in BOLD. Notably, when the interictal spikes occur at high frequency, a late hyperoxygenation is not encountered, implying that more intense epileptiform activity elicits a persistent increase in Hbr, or a metabolic demand that is never adequately met by the increase in perfusion.

Subsequent experiments by Bahar et al. (43,44) confirmed the hypothesis that prolonged epileptiform events elicit an equally prolonged state of focal hypoxia. Using 4-aminopyridine (4-AP) injections into rat neocortex, Bahar et al. recorded the IOS associated with ictal events, which lasted as long as 60 to 90 s (Fig. 3; ref. 44). ORIS at wavelengths sensitive to hemoglobin oxygenation showed a

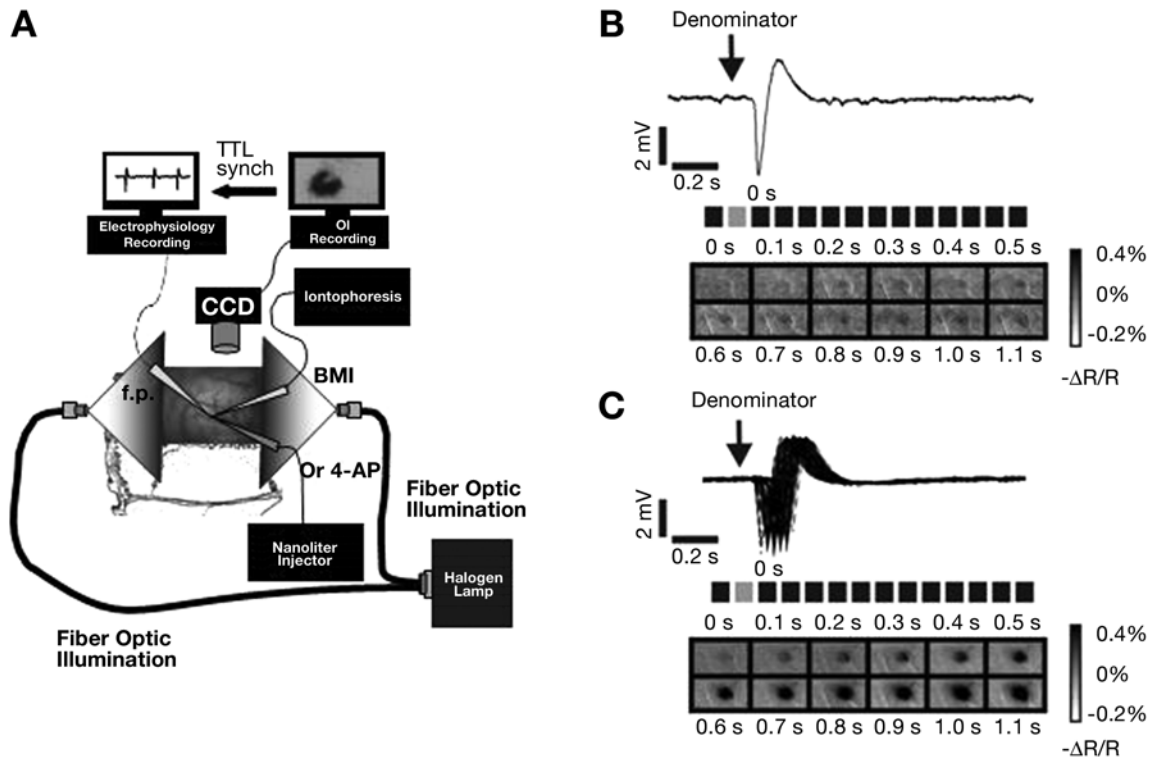


Fig. 1. Optical imaging of interictal spikes. (A) Schematic diagram of experiment for in vivo optical imaging in the rat neocortex. One side of the cranium is thinned, and a small central hole is placed down to the dura. A field potential (f.p.) electrode and an electrode for drug administration are inserted through the small hole. F.p. data are collected continuously, and images are collected simultaneously using a charge-coupled device (CCD) camera at 2 to 33 Hz temporal resolution. Both f.p. and images are stored onto a personal computer for offline analysis. (B) Spike-triggered image division of single interictal spike. A well-developed biphasic interictal spike is induced at regular interval (0.5–0.75 Hz) with focal iontophoresis of bicuculline iontophoresis electrode. ORIS map at 605 nm of single interictal spike is generated by dividing each individual frame (black bars, 100-ms frame duration) after interictal spike (IIS) by the single frame (gray bar) preceding IIS. (C) Averaging over multiple spikes ($n = 185$) increases signal-to-noise ratio. Scale bar: 1 mm.

lengthy increase in Hbr that lasted for the entire duration of the ictal event, despite a large and rapid increase in CBV (Fig. 3). Therefore, the epileptic dip is not a transient phenomenon; rather, it persists for the duration of the focal epileptiform event.

One potential criticism of this finding is the fact that the optical signal recorded at wavelengths sensitive to hemoglobin oxygenation is also partially sensitive to HbO₂. Therefore, a large increase in CBV increases Hbt, and because $Hbt = Hbr + HbO_2$, a decrease in light reflection might occur in the absence of a selec-

tive increase in Hbr. The solution is to directly measure tissue oxygenation with oxygen-sensitive electrodes.

Oxygen-Sensitive Electrodes

Clark first introduced oxygen-sensitive electrodes in the mid-1960s, when he measured partial oxygen pressure in tissue using what has become known as the "Clark-style" oxygen electrode. This electrode has a thin membrane covering a layer of electrolyte and two metallic

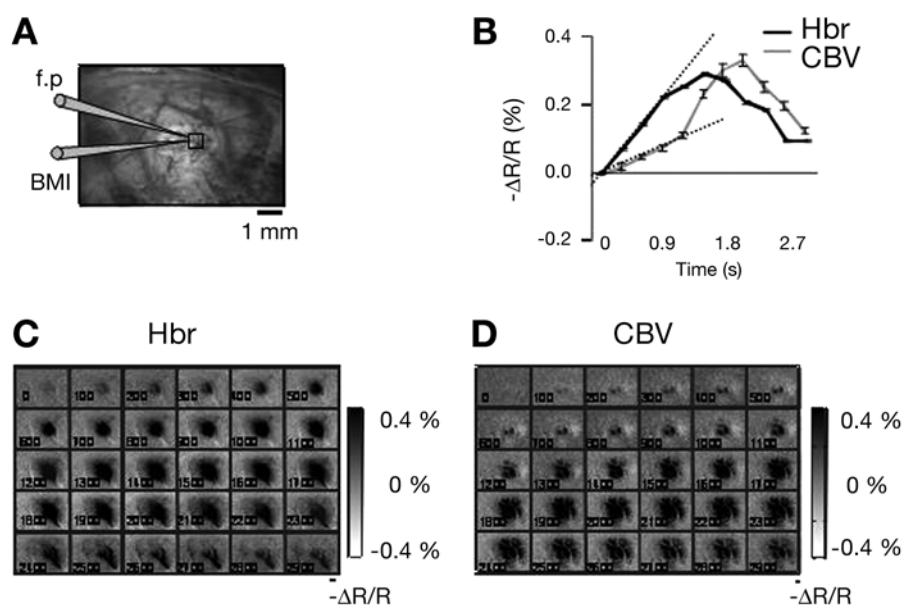


Fig. 2. ORIS map of interictal spike (IIS) at the wavelengths sensitive to CBV (546 nm) and Hbr (605 nm). (A) An image at 546 nm shows the pattern of vasculature of imaged region covered with a thin cranium. A square box is a region of interest (ROI) in the IISs focus measured in B. (B) Time-course of changes in light reflectance in the ROI measured at the wavelengths sensitive to CBV and Hbr. Error bar indicates standard deviation of pixel values in ROI. The dotted line indicates the slope of changes in light reflectance. (C,D) ORIS map of IIS at the wavelength sensitive to CBV (C; 546 nm) and Hbr (D; 605 nm). Spike-triggered image division at the wavelengths sensitive to CBV and Hbr generates ORIS map of IISs ($n = 185$ and 208, respectively). f.p., field potential electrode; BMI, bicuculline iontophoresis electrode. Scale bar: 1 mm.

electrodes that can measure partial oxygen pressure (pO_2) in brain tissue when oxygen diffuses through the membrane and is electrochemically reduced at the cathode, which is polarized against an internal anode. The greater the pO_2 , the more oxygen diffuses through the membrane and the more flow there is from the anode to the cathode, which is proportional to the amount of oxygen in brain tissue. Unlike ORIS, these Clarke-style polarographic oxygen microsensors are limited in their ability to sample only a small area of cortex. However, their temporal resolution is on the order of 100 to 500 ms. Investigators have recently applied this technique to demonstrate a small decrease in pO_2 following normal sensory processing in visual and somatosensory cortex (9,10), confirming the existence of the initial dip. However, their use of oxygen-sensitive electrodes to

measure tissue oxygenation during epileptiform events has not been reported. Recently, Zhao et al. (45) and Bahar et al. (44) measured pO_2 adjacent to a 4-AP focus in *in vivo* rat neocortex. In a series of three rats ($n =$ nine seizures), they found an immediate rapid decrease in pO_2 coincident with the onset of the seizure, followed by a gradual return to baseline (Fig. 4). The mean (standard deviation) decrease in tissue pO_2 was $64.3 \pm 23.5\%$ of baseline, with a nadir at 24 s after seizure onset. This decrease in tissue pO_2 was statistically significant from 5 to 35 s and 45 to 50 s after the onset of the seizure. These findings lend further support to the idea that focal seizures elicit an increase in $CMRO_2$ so large that the metabolic demand cannot be met by the autoregulatory mechanisms of the brain that attempt to increase CBF and CBV. It is

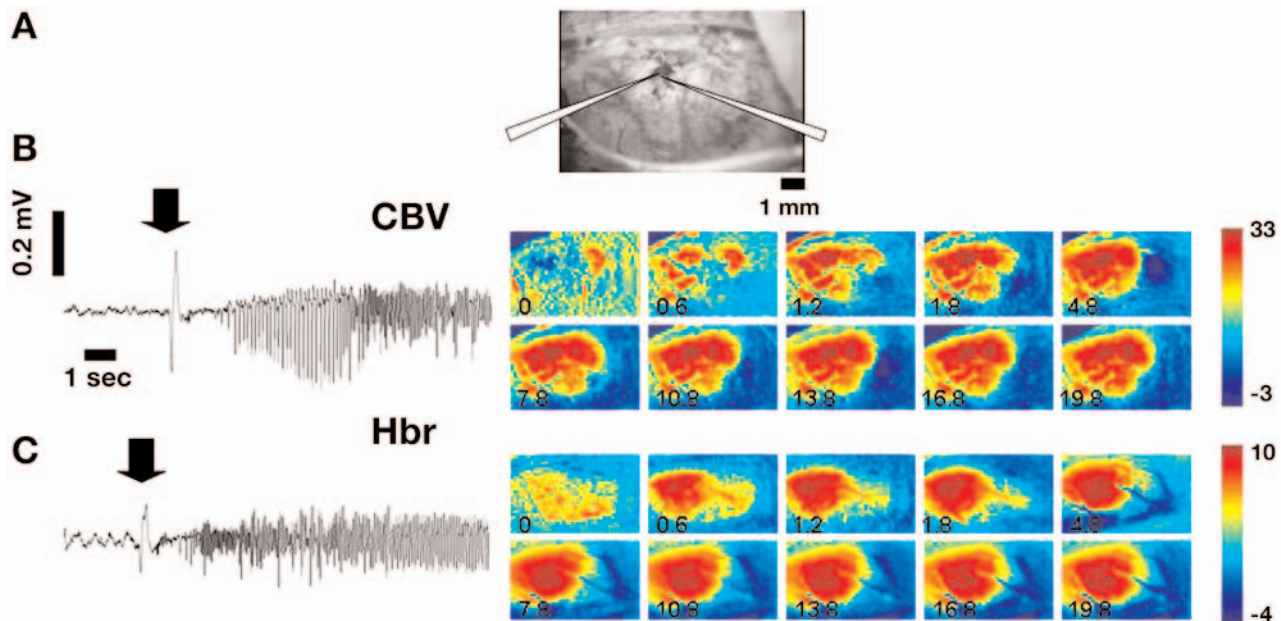


Fig. 3. Images and electrophysiology of 4-aminopyridine (4-AP) induced ictal events in an in vivo rat model. (A) An image at 546 nm shows the blood vessel pattern and locations of field potential (f.p.) and 4-AP injecting electrodes. (B) f.p. recording of single 4-AP ictal event imaged at a wavelength sensitive to CBV. Images acquired at 600 ms demonstrate ORIS map of the onset of ictal events. The single denominator frame was chosen at $t = -1.2$ s immediately before the onset ($t = 0$ s) of ictal event observed in the f.p. recording. Note the insensitivity of ORIS to subtle electrophysiology changes. There is a clear transition in f.p. recording 7 to 8 s from the onset. The images around 7 to 8 s are stable, indicating insensitivity of ORIS to changes in electrophysiology. (C) f.p. recording and ORIS map of a 4-AP ictal event imaged at the wavelength sensitive to Hbr. The single denominator frame was also chosen at $t = -1.2$ s immediately before the onset ($t = 0$ s) of the ictal event.

unknown whether this period of relative ictal and interictal ischemia are sufficient to cause transient alterations in neuronal function or even permanent tissue damage.

Cerebral Blood Volume

In response to the increased $CMRO_2$, the brain dilates arterioles, which increase Hbt. Early investigations using ORIS found that increases in CBV, unlike the initial dip, were not well-localized to the area of increased neuronal activity (4,6). Therefore, the brain spatially overperfuses metabolically active regions leading to overspill into adjacent areas. However, more recent studies have shown that CBV colocalizes with neuronal activity when measured

within the first 1 to 2 s after the neuronal event (5,46), particularly when contributions from macrovasculature can be minimized (47). These data have even more recently been confirmed using fluorescent blood plasma tracers (48). Therefore, the early CBV-related optical signal may be a useful mechanism for mapping neuronal activity, including epileptiform events. However, despite detailed studies of CBV optical mapping of normal physiological events (13,33,46–48), little is known about the focality, latency, and time-course of the brain's CBV response to epileptiform events. The few studies in this area have used techniques with poor spatial and temporal resolution such as autoradiography (19,20,22), SPECT (49), and fMRI (25–27), which have shown a dramatic, but poorly localized increase in CBF.

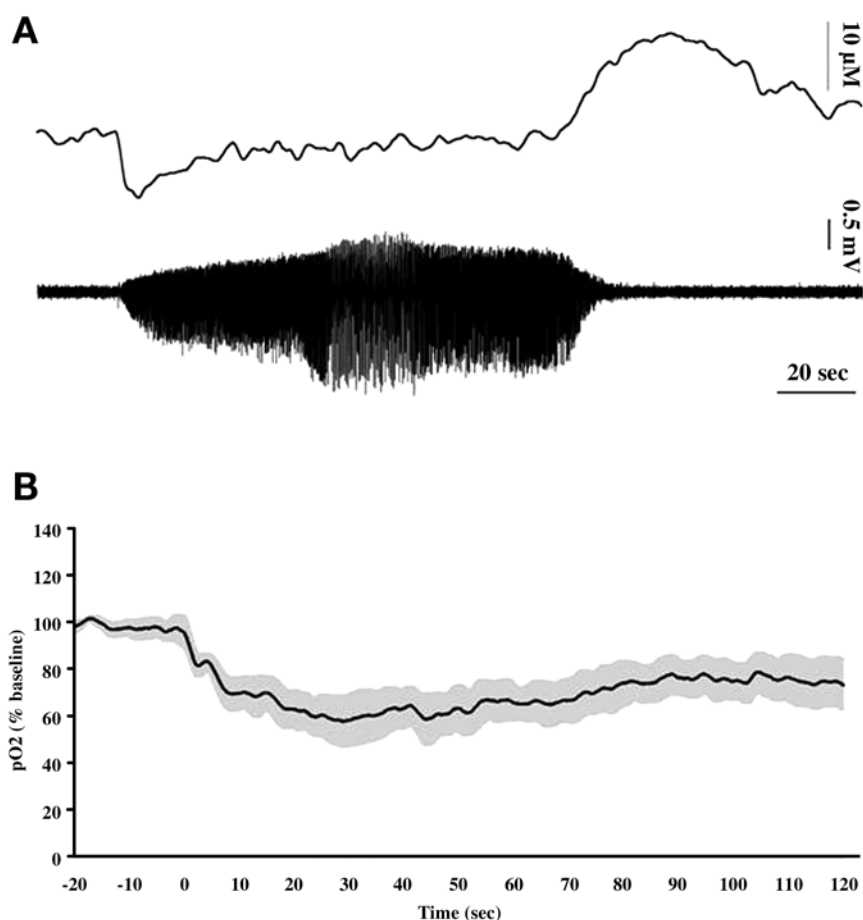


Fig. 4. Direct measurement of tissue oxygenation in acute rat model. Time-course of partial tissue oxygen (pO_2) during 4-aminopyridine induced ictal events is shown. **(A)** A typical example of pO_2 and f.p. recording of ictal event from a single animal. The onset of ictal events is defined by the peak of an initial negative spike. Decrease in tissue pO_2 is observed immediately after the onset of the ictal event. Tissue pO_2 returns to the baseline approx 45 s after the offset of the ictal event. **(B)** Average percent changes in tissue pO_2 during ictal discharges ($n = 9$ seizures, $n = 3$ animals).

Suh et al. (42) examined the CBV response to interictal spikes in vivo using ORIS with high temporal resolution (100 ms). Their results indicate that a focal change in CBV occurs within 100 to 200 ms of the interictal spike and is as equally well-localized to the pool of active neurons as the epileptic dip (Fig. 2). However, unlike the results reported for somatosensory mapping, the amplitude of the optical signal and the signal-to-noise ratio were better for the epileptic dip than the CBV response during the

first 2 s after the interictal spike. At later time-points, when the CBV signal amplitude and signal-to-noise ratio were higher than the epileptic dip, the spatial overspill of CBV rendered it less useful as a mapping signal. Therefore, the epileptic dip remains an overall better signal for mapping epilepsy, although other investigators have reported different results (50).

During ictal events, Bahar et al. (43,44) found that the increase in CBV was extremely large—an average of $13.70 \pm 9.43\%$ and in

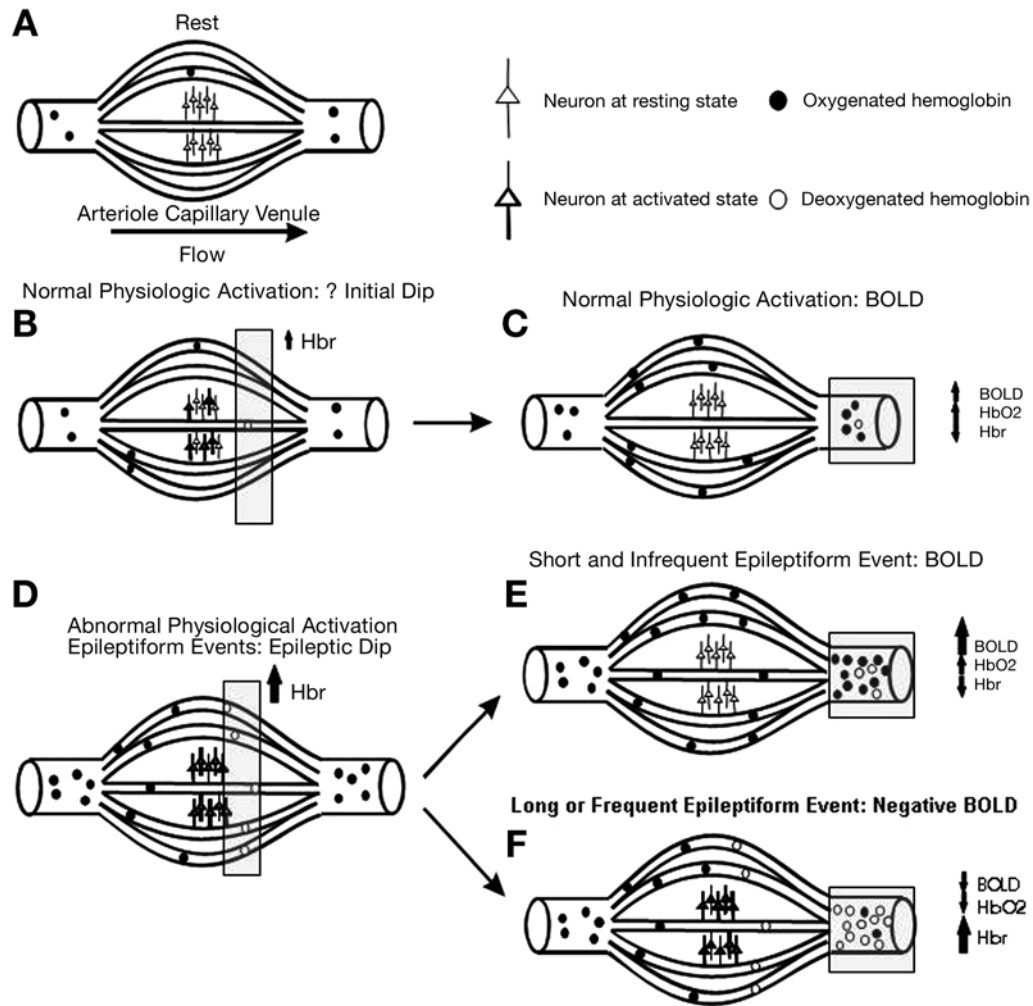


Fig. 5. Perfusion/oxygenation events following normal and abnormal cortical processing. **(A)** At rest, oxygenated hemoglobin (HbO₂) in red blood cells flows from arterioles through capillaries to venules to provide oxygen for neurons. **(B)** After normal physiological neuronal activation (darkened pyramidal cells), there is an increase in neuronal metabolism that may cause a focal increase in deoxygenated hemoglobin (Hbr), also known as the initial dip, which is seen as a decrease in reflection of light at wavelengths sensitive to hemoglobin oxygenation. **(C)** Several seconds after neuronal activation caused by normal physiological events, an increase in perfusion and CBV brings an oversupply of HbO₂, which forms the basis of the BOLD signal imaged with fMRI. This signal appears in the draining venules and may be less well-localized to the population of active neurons. **(D)** Abnormal physiological events (epileptiform events) induce a focal increase in Hbr localized to the region of active neurons (darkened pyramidal cells) because metabolism is focally increased. There is also a simultaneous focal increase in CBV. **(E)** Short or infrequent interictal epileptiform events can elicit a late BOLD signal when the increase in perfusion provides an overabundance of HbO₂. **(F)** Longer events (ictal) or more frequent interictal events have a consistently high regional metabolism that outweighs the brain's ability to increase perfusion. Therefore, a persistent increase in Hbr causes an inverted BOLD signal, which is also seen as an increase in reflection of light at a wavelength sensitive to hemoglobin oxygenation.

some situations as large as 33% (Fig. 3). However, ictal events are of long duration, lasting from several seconds to minutes, and there is a large amount of variability in the morphology of the electrical tracing, indicating shifting populations of neurons participating in the seizure. Because the IOS has relatively slow rise and decay times (on the order of several seconds—particularly at wavelengths sensitive to CBV), the IOS is a relatively poor method for mapping ictal events that shift over space and time (Fig. 3). As shown by Bahar et al. (44), despite dramatic changes in the electroencephalogram during the course of a focal seizure, the IOS remained relatively unchanged (Fig. 3B). This insensitivity emphasizes the fact that the IOS shows changes in CBV and Hbr associated with neuronal activity but not neuronal activity itself. Therefore, these optical signals can be useful for localizing the onset of a seizure but are less accurate in measuring propagation.

Epileptic Neurovascular Coupling

To summarize the data at this point, Fig. 5 presents a series of schematic cartoons. Epileptiform activity induces a dramatic increase in CMRO₂ that causes an immediate increase in Hbr and a decrease in tissue pO₂, which we call the epileptic dip. Despite a rapid increase in CBV, which is initially focal but fairly quickly (1–2 s) becomes more diffuse, tissue pO₂ remains low and Hbr remains high throughout the length of the epileptic event. Although infrequent interictal spikes are eventually followed by a late hyperoxygenation (starting ~3 s after the interictal spike), or increase in BOLD signal, more frequent interictal spikes and seizures cause a persistent increase in CMRO₂ that causes the tissue to remain slightly ischemic.

Notably, prior fMRI studies of epileptiform events do not support our hypothesis. Generally, these studies show an increase in BOLD signal associated with epilepsy (24–27). However, there are important differences in method-

ology. These fMRI studies have either examined interictal spikes using a slower temporal resolution or generalized ictal events, rather than focal events. In the former, the temporal resolution of fMRI may not be adequate to resolve the brief epileptic dip associated with interictal spikes. In the latter, neurovascular coupling associated with generalized epilepsy may not be the same as in the case of focal epilepsy, and such a widespread increase in metabolic demand may be adequately met by perfusion. Indeed, one fMRI study of more frequent and intense epileptiform events that used γ -butyrolactone to induce absence seizures showed a more prominent negative BOLD signal, consistent with a decrease in HBO₂ (51). Similarly, fluorodeoxyglucose-PET of acute rat interictal spikes has revealed hypermetabolism within the focus, particularly at high spike frequency rates (52), whereas in a more chronic model, only hypometabolism was apparent in both the focus and surround (53).

Do the Initial Dip and Epileptic Dip Exist in Human Cortex?

The translation of experimental research in rodents to the human situation has always been problematic. Human experimentation is understandably quite restricted, and invasive techniques available in the laboratory often cannot be ethically applied to humans. However, one of the advantages of ORIS is that optical recording is noninvasive once the brain has been exposed (40,54). Indeed, ORIS has been used to map epilepsy and functional architecture in humans in the context of a neurosurgical operation (41,55–59). Generally, these studies have measured light at wavelengths sensitive to LS. Therefore, there are little data on CBV and Hbr responses to cortical activation in the human. In several unpublished experiments, Suh et al. (60,61) investigated CBV and Hbr responses to bipolar cortical stimulation at varying amplitudes, both above and below the threshold to induce epileptiform-like afterdischarges.

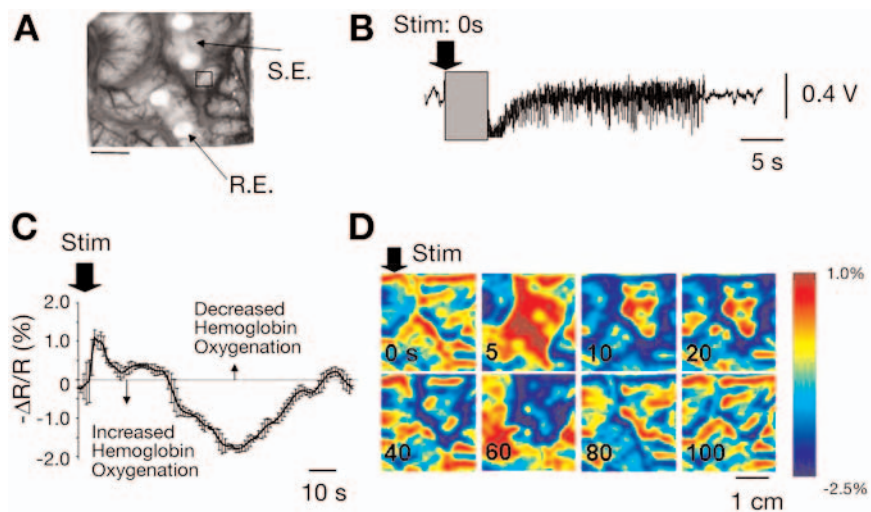
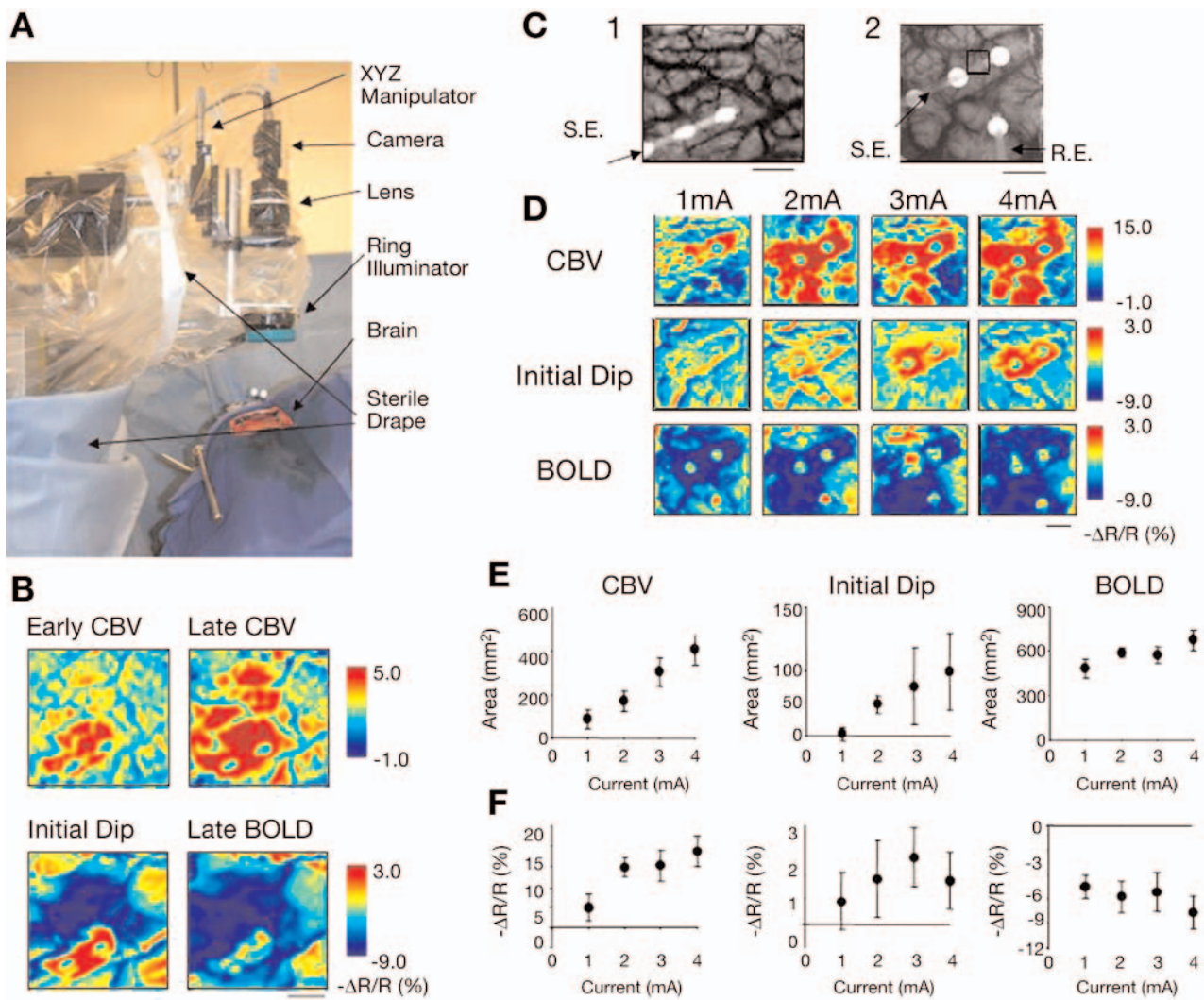


Fig. 6. Experimental setup for intra-operative human ORIS and map of direct cortical stimulation in human cortex. **(A)** Schematic diagram of experiment for intra-operative optical imaging in the human neocortex. A custom camera holder with x-y-z gross and fine manipulators suspend a camera, lens, and ring illuminator, draped in sterile plastic, over the exposed human cortex. **(B)** Intrinsic optical signals recorded at wavelengths sensitive to CBV and Hbr show that the initial focal increase in Hbr (initial dip) is more focal than the initial increase in CBV within first 2 s after the cortical stimulation. As time passes (3–5 s after the stimulation), the CBV signal spreads diffusely throughout the cortex and a dramatic inverted optical signal, consistent with the BOLD effect, appears in widespread cortical areas around the stimulating electrode. **(C)** A strip electrode is placed on the surface of the brain for direct cortical stimulation. A strip electrode for recoding EEG is outside of the field of view for patient 1 (shown in **B**) and inside of the field of view for patient 2 (shown in **D**). **(D)** ORIS maps of cortical stimulation at varying stimulus amplitudes reveal the stimulus amplitude dependence of IOS in human cortex. Highest stimulus amplitude gives the largest map of initial dip, CBV, and BOLD signals. **(E,F)** Spatial extents and changes in light reflectance of intrinsic signal at varying stimulus amplitudes are shown. An increase in stimulus amplitude causes a linear increase in the area of the initial dip and CBV signals but a nonlinear increase in BOLD signal and nonlinear increases in changes in light reflectance for all signals with a plateau effect.

In a series of eight patients who underwent craniotomy for resection of medically intractable epilepsy (approved by the Institutional Review Board at Weill Cornell Medical Center), ORIS at wavelengths sensitive to CBV and Hbr was performed during bipolar cortical stimulation at varying amplitudes. As in the animal data, following bipolar stimulation, there was a rapid (<200 ms) increase in both CBV and Hbr localized to the region beneath the electrodes. Although the initial dip remained spatially focal for several seconds, the CBV signal rapidly spread widely throughout the cortex (Fig. 6B,D). At a wavelength sensitive to Hbr, a late increase in oxygenation (reminiscent of the BOLD signal recorded with fMRI) was also recorded and was found to have poor spatial resolution, similarly to the later CBV signal. These human data confirm that the focality of

the initial dip is not temporally dependent, whereas the increase in CBV is only focal at very early time-points. On the other hand, the BOLD signal was poorly localized at all times.

Researchers also noted that at the lowest stimulation amplitude, the initial dip was almost nonexistent (Fig. 6D). As the amplitude of the stimulation was increased, there was a linear and substantial increase in the area of the initial dip and early CBV signal (Fig. 6F). On the other hand, the BOLD signal increased only slightly but still linearly. On the other hand, conversely to the area of the IOS, the amplitude of the change in light reflectance for Hbr, CBV, and BOLD varied nonlinearly with the stimulus amplitude, and a plateau effect was apparent at higher stimulation amplitudes (Fig. 6F).

The absence of the initial dip under certain experimental circumstances has been previ-

Fig. 7. Intra-operative ORIS map and the time-course of changes in light reflectance during afterdischarges. **(A)** An image at green wavelength reveals the patterns of blood vessel and stimulating and recording strip electrodes. Square box indicates the ROI for changes in pixel values. Scale bar: 1 cm. **(B)** The electrocorticography recording shows a stimulus artifact and a seizure-like afterdischarge lasting more than 20 s. Gray box indicates the duration of stimulation. **(C)** Time-course of changes in light reflectance at the wavelength sensitive to Hbr during afterdischarge shown in Fig. 9B. A profound increase in Hbr (epileptic dip) lasts more than 30 s, indicating there is a large mismatch between perfusion and metabolic demand during seizure-like afterdischarge as observed during 4-aminopyridine induced ictal events in the animal model. **(D)** ORIS map of afterdischarge in human cortex. An increase in Hbr (shown in red color) can be observed around a stimulating electrode throughout frames obtained 5 to 40 s after the cortical stimulation, followed by an inverted intrinsic signal (BOLD signal).

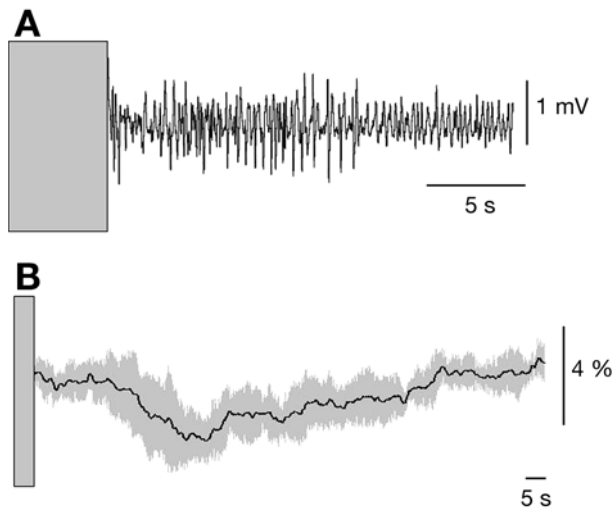


Fig. 8. Direct measurement of tissue oxygenation of human cortex during afterdischarge in human cortex. (A) The electrocorticography recording shows a stimulus artifact and a seizure-like afterdischarge. Gray box indicates the duration of stimulation (5 s). (B) Averaged percent changes in tissue pO₂ during afterdischarges ($n = 4$) from a single patient. Gray bar indicates the duration of stimulation and error bars (gray line) in graph indicate the standard deviation.

ously observed, leading some investigators to question its existence or attribute its presence to unique anesthetic conditions (14,62). Another explanation, supported by these data, is the presence of a tissue oxygen buffer that reduces the need to extract oxygen from hemoglobin at low levels of synaptic activity (63,64). More intense cortical activity, such as epilepsy, overwhelms the buffer, requiring oxygen extraction from adjacent capillaries. Indeed, studies in animals in which degrees of peripheral sensory stimulation have been applied have confirmed the graded response of the initial dip (9,13,33,65). Finally, the plateau effect observed at high stimulation amplitudes may represent a similar plateau in the number of recruited neurons at higher levels of stimulation, which has been demonstrated in rats with direct cortical stimulation (66).

High-amplitude cortical stimulation can induce ictal-like afterdischarges. ORIS in human

cortex during these electrically triggered epileptiform events reveals a persistent increase in Hbr, mirroring the animal seizure data (Fig. 7). The duration of the increase in Hbr was significantly longer (t -test; $p < 0.05$) than the increase that occurred during lower amplitude cortical stimulation that did not elicit afterdischarges, and it persisted for the duration of the event (~20 s; ref. 67). Therefore, the epileptic dip is not just a rodent phenomenon but clearly exists in humans as well, at least during focal epileptiform events. These results were then confirmed with an oxygen-sensitive electrode approved by the Food and Drug Administration for use in humans (LICOX; Integra Neuroscience). Although the T90 (latency for 90% of signal to reach sensor) for this probe is quite long (~90 s), a clear decrease in tissue oxygenation has been recorded following stimulation-induced afterdischarges (Fig. 8).

Voltage-Sensitive Dyes

The ability to map neuronal activity noninvasively—albeit indirectly—with IOS has engendered interest in using this technique for mapping both normal and abnormal functional architecture in humans during neurosurgical procedures to guide brain operations (40,54). However, for this technique to be useful, the correlation between the IOS and the underlying neuronal activity must be well understood. Studies in laboratory animals have shown that the IOS measures hemodynamic changes in a much larger area of cortex than the population of spiking neurons (31,68) and, more likely, correlates with the area of either multiunit activity recorded with field potential electrodes or synaptic activity recorded with VSDs. (31,69,70).

VSDs are a group of molecular probes that can monitor changes in membrane potential in a large area of cortex simultaneously with extremely high temporal resolution (<1 ms). VSDs bind to the external plasma membrane and change fluorescence in response to changes in transmembrane voltage (71). Signals reflect

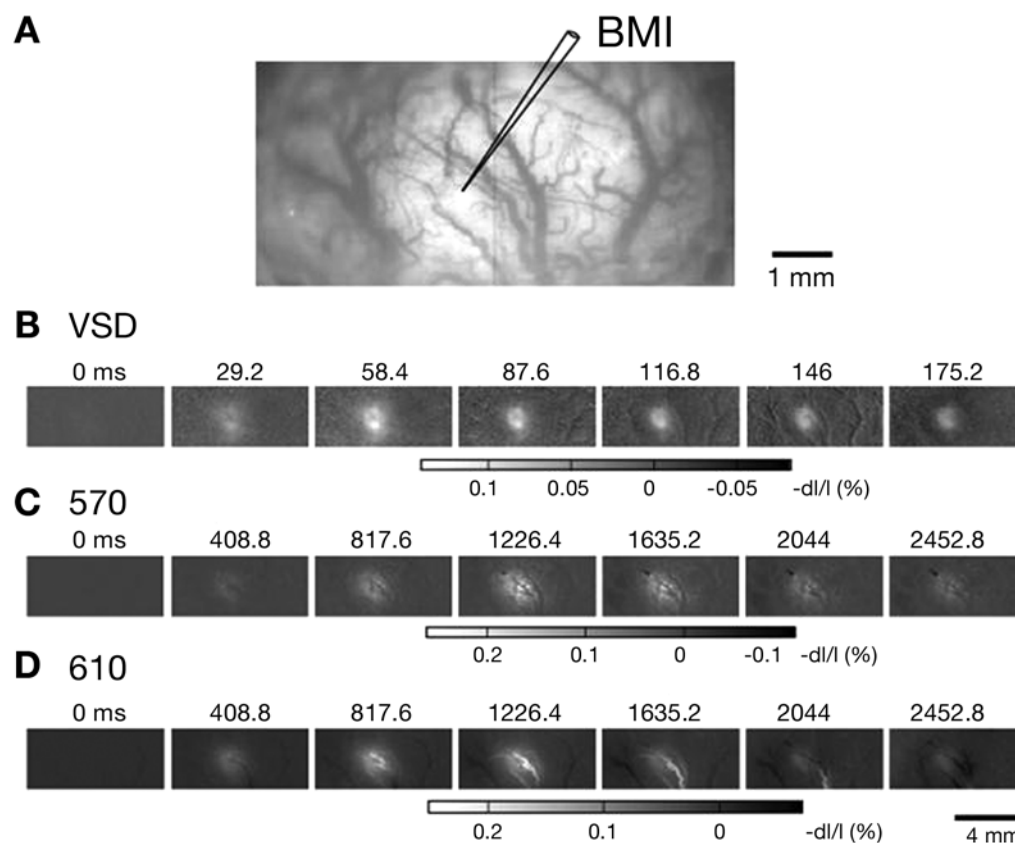


Fig. 9. IOS and VSD map of interictal spikes (IISs) from the same animal. **(A)** An image at green wavelength reveals the pattern of blood vessel and the location of bicuculline electrode. **(B)** The VSD map of IISs. Note the early onset and focality of VSD signals. **(C,D)** The ORIS maps are obtained at wavelengths sensitive to CBV (570 nm) and Hbr (610 nm) from the same animal used for VSD imaging. Note the delay in the hemodynamic response compared with the change in membrane voltage.

summated activity of populations of cells (anywhere from hundreds to thousands, depending on the size of the detector; ref. 72). Because most of the membrane in the neocortex exists in the dendrites of pyramidal cells, this activity comprises the majority of the signal (10,73,74). Blocking postsynaptic receptors shows that a large component of this signal is presynaptic (75).

VSDs have been applied to the study of epilepsy *in vitro* (67,72–74,76) and *in vivo* (77,78) to map the initiation and propagation of the interictal and ictal events. However, no studies have examined the correlation between the VSD signal and the IOS during epilepsy. This infor-

mation is critical to understanding how to use the IOS in humans to map epileptiform events in preparation for surgical treatment.

Ma et al. (79) recorded VSD and IOS during bicuculline-induced interictal spikes *in vivo* in rat neocortex. Interictal spikes induced a focal change in membrane potential that could be mapped and thresholded (3 standard deviations above the mean) to indicate the area of excitatory synaptic activity. Sequential ORIS at 570 and 610 nm were used to map the area of CBV and Hbr, respectively. Two-dimensional cross-correlations were performed to find the latency and wavelength that provided the

highest correlation between the two signals. Their results indicated that the IOS at the time-point when the signal amplitude was at its maximum overspilled the VSD map of membrane potential by approx 130%. Therefore, the increase in CBV and decrease in pO₂ occur not just in the epileptic focus but also in the cortex surrounding the focus, which has been shown to be inhibitory. It is likely that even inhibitory activity elicits an overall increase in CMRO₂ because interneurons fire more rapidly to decrease pyramidal cell activity. Additionally, the highest correlation between VSD and IOS signals occurred early in the development of the epileptic dip ($r = 0.68$ at ~650 ms). The CBV signal also correlated well at early time-points ($r = 0.62$ at ~1200 ms); however, the correlation coefficient was lower, and the latency was longer (Fig. 9). Therefore, the earliest and highest correlation occurred using the Hbr signal or epileptic dip. These findings are critical for future clinical applications of the IOS as a therapeutic adjunct in epilepsy surgery.

Conclusions

As the temporal and spatial resolution of optical imaging techniques has improved, so too has our understanding of neurovascular coupling during epileptiform events. Although epilepsy is an abnormal brain state, the hemodynamic response of the brain follows patterns similarly to normal cortical processing. The dip in hemoglobin oxygenation, which is found inconsistently following normal cortical activity, becomes much larger and more consistent during epileptiform events and can last for minutes, depending on the length of the ictus. However, acute pharmacologically induced focal epilepsy may induce a much greater increase in CMRO₂ compared with human epilepsy, and general anesthesia may impair cerebral autoregulation. The epileptic dip is also present in humans under similar circumstances to supranormal focal brain activation. Whether the chronically epileptic human brain experiences an ictal dip in oxygenation is not

known. Histological evidence for ischemic damage associated with chronic epilepsy is controversial, depending on the type and duration of epilepsy and method of histological analysis. Hopefully, the development of newer noninvasive methods for measuring neuronal and cerebrovascular dynamics with improved spatial and temporal resolution in the human will shed further light on these important questions.

Acknowledgments

This work was supported by grants to T. H. Schwartz from the Epilepsy Foundation Research Clinical Training Fellowship, Alexander von Humboldt Foundation, Van Wagenen Fellowship (AANS), Young Clinician Investigator Award (AANS), Epilepsy Fellowship Junior Investigator Award, Citizens United for Research in Epilepsy (CURE), Dana Foundation Program in Clinical Imaging, NINDS (K08 NS 43799, R21 NS 42325, R01 NS 94822). We gratefully acknowledge Koon-Ho Danny Wong for technical assistance.

References

1. Roy C. and Sherrington C. (1890) On the regulation of the blood supply to the brain. *J. Physiol. Lond.* **11**, 85–108.
2. Fox P. T., Raichle M. E., Mintun M. A., and Dence C. (1988) Nonoxidative glucose consumption during focal physiologic neural activity. *Science* **241**, 462–464.
3. Ogawa S., Lee T. M., Kay A. R., and Tank D. W. (1990) Brain magnetic resonance imaging with contrast dependent on blood oxygenation. *Proc. Natl. Acad. Sci. USA* **87**, 9868–9872.
4. Frostig R. D., Lieke E. E., Ts'o D. Y., and Grinvald A. (1990) Cortical functional architecture and local coupling between neuronal activity and the microcirculation revealed by in vivo high-resolution optical imaging of intrinsic signals. *Proc. Natl. Acad. Sci. USA* **87**, 6082–6086.
5. Sheth S. A., Nemoto M., Guiuo M., Walker M., Pouratian N., and Toga A. W. (2003) Evaluation of coupling between optical intrinsic signals

- and neuronal activity in rat somatosensory cortex. *NeuroImage* **19**, 884–894.
6. Malonek D. and Grinvald A. (1996) Interactions between electrical activity and cortical microcirculation revealed by imaging spectroscopy: implications for functional brain mapping. *Science* **272**, 551–554.
 7. Mayhew J. E. W., Zheng Y., Hou Y., et al. (1999) Spectroscopic analysis of changes in remitted illumination: the response to increased neural activity in brain. *NeuroImage* **10**, 304–326.
 8. Vanzetta I. and Grinvald A. (1999) Increased cortical oxidative metabolism due to sensory stimulation: implications for functional brain imaging. *Science* **286**, 1555–1558.
 9. Thompson J. K., Peterson M. R., and Freeman R. D. (2003) Single-neuron activity and tissue oxygenation in the cerebral cortex. *Science* **299**, 1070–1072.
 10. Ances B. M., Buerk D. G., Greenberg J. H., and Detre J. A. (2001) Temporal dynamics of the partial pressure of brain tissue oxygen during functional forepaw stimulation in rats. *Neurosci. Lett.* **306**, 106–110.
 11. Logothetis N. K., Guggenberger H., Peled S., and Pauls J. (1999) Functional imaging of the monkey brain. *Nature Neurosci.* **2**(6), 555–562.
 12. Kim D.-S., Duong T. Q., and Kim S.-G. (2000) High-resolution mapping of iso-orientation columns by fMRI. *Nature Neurosci.* **3**(2), 164–169.
 13. Sheth S. A., Nemoto M., Guioi G., Walker M., Pouratian N., and Toga A. W. (2004) Linear and nonlinear relationships between neuronal activity, oxygen metabolism, and hemodynamic response. *Neuron* **42**, 347–355.
 14. Vanzetta I. and Grinvald A. (2001) Evidence and lack of evidence for the initial dip in the anesthetized rat: implications for human functional brain imaging. *NeuroImage* **13**, 959–967.
 15. Lindauer U., Royle G., Leithner C., et al. (2001) No evidence for early decrease in blood oxygenation in rat whisker cortex in response to functional activation. *NeuroImage* **13**, 988–1001.
 16. Folbergrova J., Ingvar M., and Siesjö B. K. (1981) Metabolic changes in cerebral cortex, hippocampus, and cerebellum during sustained bicuculline-induced seizures. *J. Neurochem.* **37**, 1228–1238.
 17. Bragin A., Mody I., Wilson C. L., and Engel J. J. (2002) Local generation of fast ripples in epileptic brain. *J. Neurosci.* **22**, 5, 2012–2021.
 18. de Curtis M. and Avanzini G. (2001) Interictal spikes in focal epileptogenesis. *Prog. Neurobiol.* **63**, 541–567.
 19. Pereira de Vasconcelos A., Ferrandon A., and Nehlig A. (2002) Local cerebral blood flow during lithium-pilocarpine seizures in the developing and adult rat: role of coupling between blood flow and metabolism in the genesis of neuronal damage. *J. Cereb. Blood Flow Metab.* **22**, 196–205.
 20. Andre V., Henry D., and Nehlig A. (2002) Dynamic variations of local cerebral blood flow in maximal electroshock seizures in the rat. *Epilepsia* **43**, 1120–1128.
 21. Ingvar M. (1986) Cerebral blood flow and metabolic rate during seizures: relationship to epileptic brain damage. *Ann. NY Acad. Sci.* **462**, 207–223.
 22. Tanaka S., Sako K., Tanaka T., Nishihara I., and Yonemasu Y. (1990) Uncoupling of local blood flow and metabolism in the hippocampal CA3 kainic acid-induced limbic seizure status. *Neuroscience* **36**, 339–348.
 23. Kreisman N. R., Magee J. C., and Brizzee B. L. (1991) Relative hypoperfusion in rat cerebral cortex during recurrent seizures. *J. Cereb. Blood Flow Metab.* **11**, 77–87.
 24. Tenney J. R., Duong T. Q., King J. A., and Ferris C. F. (2004) FMRI of brain activation in genetic rat model of absence seizures. *Epilepsia* **45**, 6, 576–582.
 25. Nersesyan H., Hyder F., Rothman D. L., and Blumenfeld H. (2004) Dynamic fMRI and EEG recording during Spike-Wave seizures and generalized tonic-clonic seizures in WAG/Rij rats. *J. Cereb. Blood Flow Metab.* **24**, 589–599.
 26. Lemieux L., Krakow K., and Rife D. R. (2001) Comparison of spike-triggered functional MRI BOLD activation and EEG dipole model localization. *NeuroImage* **14**, 1097–1104.
 27. Benar C.-G., Goross D. W., Wang Y., et al. (2002) The BOLD response to interictal epileptiform discharges. *NeuroImage* **17**, 1182–1192.
 28. Hill D. K. and Keynes R. D. (1949) Opacity changes in stimulated nerve. *J. Physiol.* **108**, 278–281.
 29. Schwartz T. H., Chen L.-M., Friedman R. M., Spencer D. D., and Roe A. W. (2004) High resolution intraoperative optical imaging of human face cortical topography: a case study. *NeuroReport* **15**, 9, 1527–1531.
 30. Bonhoeffer T. and Grinvald A. (1991) Iso-orientation domains in cat visual cortex are arranged in pinwheel-like patterns. *Nature* **353**, 429–431.
 31. Bonhoeffer T. and Grinvald A. (1996) The Methods, in Brain Mapping, Toga A. W. and Mazziotta J. C., eds., 55–99, San Diego: Academic.

32. Mayhew J. E. W., Johnston D., Berwixk J., Jones M., Cofey P. and Zheng Y. (2000) Spectroscopic analysis of neural activity in brain: increased oxygen consumption following activation of barrel cortex. *NeuroImage* **12**, 664–675.
33. Nemoto M., Sheth S., Guiou M., Pouratian N., Chen J. W. Y., and Toga A. W. (2004) Functional signal- and paradigm-dependent linear relationships between synaptic activity and hemodynamic responses in rat somatosensory cortex. *J. Neurosci.* **24**, 15, 3850–3861.
34. Sato C., Nemoto M., and Tamura M. (2002) Reassessment of activity-related optical signals in somatosensory cortex by an algorithm with wavelength-dependent path length. *Jpn. J. Physiol.* **52**, 301–312.
35. Hochman D. W., Baraban S. C., Owens J. W. M., and Schwartzkroin P. A. (1995) Dissociation of synchronization and excitability in furosemide blockade of epileptiform activity. *Science* **270**, 99–102.
36. Federico P., Borg S. G., Salkauskus A. G., and MacVicar B. A. (1994) Mapping patterns of neuronal activity and seizure propagation in the isolated whole brain of the guinea-pig. *Neuroscience* **58**, 3, 461–480.
37. Chen J. W. Y., O'Farrell A. M., and Toga A. W. (2000) Optical intrinsic signal imaging in a rodent seizure model. *Neurology* **55**, 312–315.
38. Schwartz T. H. and Bonhoeffer T. (2001) In vivo optical mapping of epileptic foci and surround inhibition in ferret cerebral cortex. *Nature Med.* **7**(9), 1063–1067.
39. Schwartz T. H. (2003) Optical imaging of epileptiform events in visual cortex in response to patterned photic stimulation. *Cereb. Cortex* **13**, 12, 1287–1298.
40. Schwartz T. H. (2005) The application of optical recording of intrinsic signal to simultaneously acquire functional, pathological and localizing information and its potential role in neurosurgery. *Stereotac. Funct Neurosurg.* **83**, 36–44.
41. Haglund M. M., Ojemann G. A., and Hochman D. W. (1992) Optical imaging of epileptiform and functional activity in human cerebral cortex. *Nature* **358**(6388), 668–671.
42. Suh M., Bahar S., Mehta A. D., and Schwartz T. H. (2005) Temporal dependence in uncoupling of blood volume and oxygenation during interictal epileptiform events in rat neocortex. *J. Neurosci.* **25**, 1, 68–77.
43. Bahar S., Suh M., Mehta A. D., and Schwartz T. H. (2005) In Bioimaging in Neurodegeneration, Broderick P. A., Rahni D. N., and Kolodny E. H., eds., Totowa, NJ: Humana Press, pp. 149–175.
44. Bahar S., Suh M., and Schwartz T. H. (2006) Intrinsic optical signal imaging of neocortical seizures: the “epileptic dip.” *Neuroreport* **19**(5), 499–503.
45. Zhao M., Ma H., Suh M., and Schwartz T. H. (2005) Decrease in brain tissue oxygenation in spite of an increase in cerebral blood flow during acute focal 4-aminopyridine seizures in rat neocortex. Abstract for Society of Neuroscience Annual Conference, November 12–16.
46. Sheth S. A., Nemoto M., Guiou G., et al. (2004) Columnar Specificity of microvascular oxygenation and volume responses: Implications for functional brain mapping. *J. Neurosci.* **24**(3), 634–641.
47. Vanzetta I., Sloviter H., Omer D. B., and Grinvald A. (2004) Columnar resolution of blood volume and oximetry functional maps in the behaving monkey: Implications for fMRI. *Neuron* **42**, 843–854.
48. Vanzetta I., Hildesheim R., and Grinvald A. (2005) Compartment-resolved imaging of activity dependent dynamics of cortical blood volume and oximetry. *J. Neurosci.* **25**(9), 2233–2244.
49. Van Paesschen W. (2004) Ictal SPECT. *Epilepsia* **45**(S4), 35–40.
50. Haglund M. M. and Hochman D. W. (2004) Optical imaging of epileptiform activity in human neocortex. *Epilepsia* **45**(S4), 43–47.
51. Tenney J. R., Duong T. Q., King J. A., and Ferris C. F. (2003) Corticothalamic modulation during absence seizures in rats: a functional MRI assessment. *Epilepsia* **44**, 1133–1140.
52. Handforth A., Finch D. M., Peters R., Tan A. M., and Treiman D. M. (1994) Interictal spiking increases 2deoxy[14C]glucose uptake and c-fos-like reactivity. *Ann. Neurol.* **35**, 724–731.
53. Hagemann G., Bruehl C., Lutzenburg M., and Wite O. W. (1998) Brain hypometabolism in a rat model of chronic focal epilepsy in rat neocortex. *Epilepsia* **39**(4), 339–346.
54. Pouratian N., Sheth S. A., Martin N. A., and Toga A. W. (2003) Shedding light on brain mapping: advances in human optical imaging. *Trends Neurosci.* **26**(5), 277–282.
55. Schwartz T. H., Chen L. M., Friedman R. M., Spencer D. D., and Roe A. W. (2005) Intraoperative optical imaging of human face cortical topography: a case study. *NeuroReport* **15**(9), 1527–1531.
56. Cannestra A. F., Black K. L., Martin N. A., et al. (1998) Topographical and temporal specificity

- of human intraoperative optical intrinsic signals. *NeuroReport* **9**, 2557–2563.
57. Cannestra A. F., Pouratian N., Bookheimer S. Y., Martin N. A., Becker D. P., and Toga A. W. (2001) Temporal spatial differences observed by functional MRI and human intraoperative optical imaging. *Cerebral Cortex* **11**, 773–782.
 58. Sato K. et al. (2002) Intraoperative intrinsic signal imaging of neuronal activity from subdivisions of the human primary somatosensory cortex. *Cerebral Cortex* **12**, 269–280.
 59. Shoham D. and Grinvald A. (2001) The cortical representation of the hand in macaque and human area S-1: high resolution optical imaging. *J. Neurosci.* **21**, 17, 6820–6835.
 60. Suh M., Bahar S., Mehta, A. D., and Schwartz T. H. (2006) Blood volume and hemoglobin oxygenation response following electrical stimulation of human cortex. *Neuroimage*, in press.
 61. Suh M., Bahar S., Mehta A. D., et al. (2005) Optical imaging of intrinsic signal during stimulus-induced afterdischarge in the human cortex. *Soc. Neurosci. Abs.*
 62. Lindauer U., Gethman J., Kuhl M., Kohl-Bareis M., Villringer A., and Dirnagl U. (2003) Neuronal activity-induced changes of local cerebral microvascular blood oxygenation in the rat: effect of systemic hyperoxia or hypoxia. *Brain Res.* **975**, 135–140.
 63. Buxton R. B. (2001) The elusive initial dip. *NeuroImage* **13**, 953–958.
 64. Buxton R. B., Wong E. C., and Frank L. R. (1998) Dynamics of blood flow and oxygenation changes during brain activation: the balloon model. *Magn. Res. Med.* **39**, 855–864.
 65. Jones M., Berwick J., Johnston D., and Mayhew J. E. W. (2001) Concurrent optical imaging spectroscopy and laser-doppler flowmetry: the relationship between blood flow, oxygenation, and volume in rodent barrel cortex. *NeuroImage* **13**, 1002–1015.
 66. Butovas S. and Schwarz C. (2003) Spatiotemporal effects of microstimulation in rat neocortex: a parametric study using multielectrode recordings. *J. Neurophysiol.* **90**, 3024–3039.
 67. Sutor B., Hablitz J. J., Rucker F., and Bruggen-cate G. (1994) Spread of epileptiform activity in the immature rat neocortex studied with voltage-sensitive dyes and laser scanning microscopy. *J. Neurophys.* **4**, 1756–1768.
 68. Das A. and Gilbert C. D. (1995) Long-range horizontal connections and their role in cortical reorganization revealed by optical recording of cat primary visual cortex. *Nature* **375**, 780–784.
 69. Takashima I., Kajiwarra R., and Iijima T. (2001) Voltage-sensitive dye versus intrinsic signal optical imaging: comparison of optically determined functional maps from rat barrel cortex. *Neuroreport* **12**, 13, 2889–2894.
 70. Logothetis N. K., Pauls J., Augath M., Trinath T., and Oeltermann A. (2001) Neurophysiological investigation of the basis of the MRI signal. *Nature* **412**, 150–157.
 71. Grinvald A., Frostig R. D., Lieke E., and Hildesheim R. (1988) Optical imaging of neuronal activity. *Physiol. Rev.* **68**, 1285–1365.
 72. Tsau Y., Guan L., and Wu J.-Y. (1998) Initiation of spontaneous epileptiform activity in the neocortical slice. *J. Neurophysiol.* **80**, 978–982.
 73. Albowitz B. and Kuhnt U. (1995) Epileptiform activity in the guinea-pig neocortical slice spreads preferentially along supragranular layers-recordings with voltage-sensitive dyes. *Europ. J. Neurosci.* **7**, 1273–1284.
 74. Albowitz B., Kuhnt U., and Ehrenreich L. (1990) Optical recording of epileptiform voltage changes in the neocortical slice. *Exp. Brain. Res.* **81**, 241–256.
 75. Yuste R. M., Simons D. J., and Woolsey T. A. (1997) The neocortical local circuit—a research workshop held in Sde-Boker, Israel, May 4–8, 1997. *Somatosens Mot Res.* **14**(3), 213–221.
 76. Tsau Y., Guan L., and Wu J.-Y. (1999) Epileptiform activity can be initiated in various neocortical layers: an optical imaging study. *J. Neurophysiol.* **82**, 1965–1973.
 77. London J. A., Cohen L. B., and Wu J.-Y. (1989) Optical recordings of the cortical response to whisker stimulation before and after the addition of an epileptic agent. *J. Neurosci.* **9**(6), 2182–2190.
 78. Ma H., Wu C. H., and Wu JY. (2004) Initiation of spontaneous epileptiform events in the rat neocortex in vivo. *J Neurophysiol.* **91**(2), 934–945.
 79. Ma H., Zhao M., Shariff S., Wong K., Suh M., and Schwartz T. H. (2005) The Spatial Correlation between Neuronal Activity and Intrinsic Optical Signals during Interictal Spikes in Rat Neocortex. *Soc. Neurosci. Ann. Conf.*
 80. McKhann G. M. 2nd, Schoenfeld-McNeill J., Born D. E., Haglund M. M., and Ojemann G. A. (2000) Intraoperative hippocampal electrocorticography to predict the extent of hippocampal resection in temporal lobe epilepsy surgery. *J Neurosurg.* **93**(1), 44–52.